Title

Divergent Asymmetric Synthesis of Panowamycins, TM-135, and Veramycin F Using C−H Insertion with Donor/Donor Carbenes

Journal

Angewandte Chemie International Edition, 61(25)

ISSN

1433-7851

Authors

Bergstrom, Benjamin D
Merrill, Amy T
Fettinger, James C
et al.

Publication Date

2022-06-20

DOI

10.1002/anie.202203072

Peer reviewed

HHS Public Access

Author manuscript

Angew Chem Int Ed Engl. Author manuscript; available in PMC 2023 June 20.

Published in final edited form as:

Angew Chem Int Ed Engl. 2022 June 20; 61(25): e202203072. doi:10.1002/anie.202203072.

Divergent Asymmetric Synthesis of Panowamycins, TM-135, and Veramycin F using C–H Insertion with Donor/Donor Carbenes

Benjamin D. Bergstrom[a], **Dr. Amy T. Merrill**[b], **Dr. James C. Fettinger**[c], **Dean J. Tantillo**[b] **[Prof.]**, **Jared T. Shaw**[a] **[Prof.]**

[a]Department of Chemistry, University of California, Davis, One Shields Ave., Davis, CA 95161 USA

[b]Department of Chemistry, University of California, Davis, One Shields Ave., Davis, CA 95161 USA

[c]Department of Chemistry, University of California, Davis, One Shields Ave., Davis, CA 95161 USA

Abstract

Panowamycins are a group of isochroman-based natural products first isolated from *Streptomyces* sp. K07–0010 in 2012 by Satoshi Ōmura and coworkers that exhibit modest anti-trypanosomal activity. Herein we demonstrate the first syntheses of these natural products, their epimers. Stereoselective dirhodium-catalyzed C–H insertion reactions with a donor/donor carbene construct the substituted isochroman core in the key bond-forming step. The syntheses are completed without the use of protecting groups and feature a late-stage Wacker oxidation. Incongruent NMR spectra between natural and synthetic samples revealed the structural misassignment of panowamycin A and veramycin F. Computational NMR studies suggested panowamycin A to be an alternate diastereomer, which was confirmed by synthesizing this isomer. Concurrent with this work, in 2021 Mahmud and coworkers came to the same conclusion with an updated NMR analysis of panowamycin A. In a divergent, asymmetric sequence, we report the synthesis of panowamycin A, panowamycin B, TM-135, and veramycin F.

Entry for the Table of Contents

Institute and/or researcher Twitter usernames: J.T. Shaw jtshaw@ucdavis.edu.

Supporting information for this article is given via a link at the end of the document.

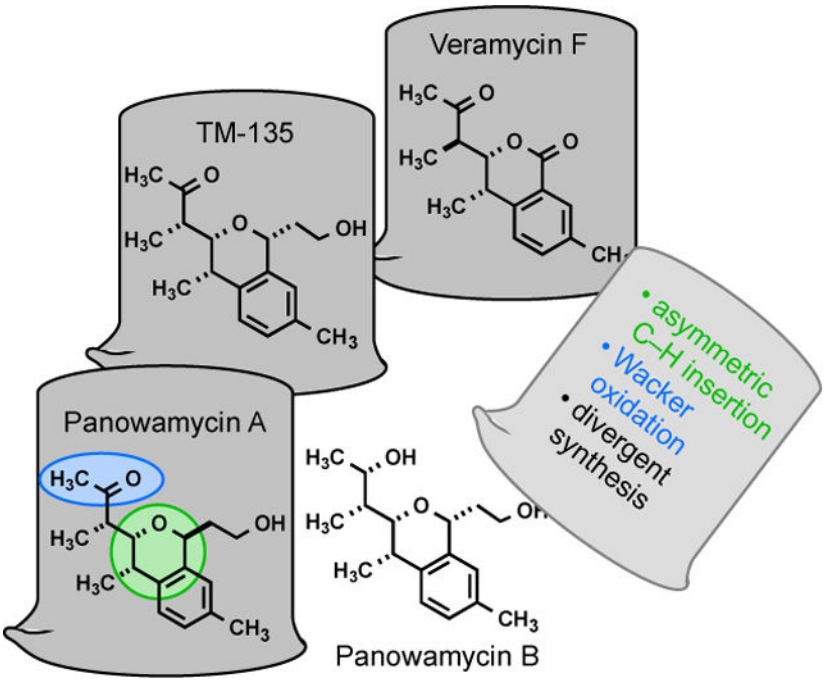

Total Synthesis Shell Game: the asymmetric first synthesis of panowamycin A, panowamycin B, TM-135, veramycin F, and two unnatural isomers in a stereoselective fashion, featuring a dirhodium-catalyzed C–H insertion reaction with donor/donor carbenes in the key step to construct the isochroman core. These syntheses reveal a structural misassignment for panowamycin A and computational NMR studies unveil the correct configuration of the natural isomer, which was also synthesized.

Keywords

asymmetric catalysis; C–H insertion; donor/donor carbene; total synthesis

Isochromans are found as the core structure of several natural products and biologically relevant molecules.[1–8] In 2012, Ōmura and coworkers, as part of their program for discovering treatments for infectious tropical diseases, isolated panowamycin A (**1**) and B (**2**), containing a novel, poly-substituted isochroman scaffold from a culture of *Streptomyces* sp. K07–0010 (Figure 1).[9] Known *Streptomyces* metabolite NFAT-133 (**6**) was also isolated in this work and appeared to be related to the panowamycins, benwamycins, and veramycins.[8,10,11] The polyketide natural product **6** has been the subject of several publications resulting in the unambiguous determination of its relative and absolute configuration.[11,12] Recently, Mahmud and coworkers have determined the biosynthetic pathway to NFAT-133 and, in a more recent publication, have proposed a revised relative and absolute structure for panowamycin A (**3**) based on updated NMR analysis and CD spectroscopy.[13,14] In their report, they posit that an intramolecular alkoxylation of the styrene of NFAT-133 from either the *si* or *re* face can proceed to form panowamycin A (**3**) or TM-135 (**4**), respectively. Both of these compounds were isolated from their fermentation of *Streptomyces pactum* ATCC 27456. As our work was largely complete prior to the report

by Mahmud and coworkers, below we will focus on our independent findings, followed by a comparison of our respective conclusions. In this way, we unambiguously confirm the relative and absolute configuration of panowamycin A (**3**) and TM-135 (**4**), and assign the relative and absolute configuration of panowamycin B (**5**) by asymmetric synthesis, in addition to synthesizing two unnatural epimers and the recently reported veramycin F (**46**).

To date, very few methods exist to construct isochromans stereoselectively.[15–17] Asymmetric variants of the oxa-Pictet Spengler reaction have achieved high levels of enantioselectivity at the isochroman C3.[18,19] Carbene insertion reactions into ether C–H bonds have been shown to be powerful tools in constructing complex chiral molecules, with foundational intramolecular work by Doyle and Davies,[20–22] and intermolecular work by Davies.[23,24] Previous work to construct chroman scaffolds with acceptor-substituted carbenes have the liability of competing Stevens rearrangement.[25,26] Recently, our lab has demonstrated that donor/donor rhodium carbenes offer excellent reactivity, chemo-, regio-, diastereo-, and enantioselectivity when applied to the synthesis of isochromans by intramolecular C–H insertion reactions.[27] Specifically, our method provides a single *cis*-diastereomer at C10 and C11 in all cases with high enantioselectivity and without competing Stevens rearrangement. As such, this method provides an excellent strategy for synthesizing the panowamycins and offers some benefits over traditional approaches in polyketide natural products synthesis; most notably, it avoids the use of chiral auxiliaries (Figure 2A).[8,11,28]

Two retrosynthetic strategies were initially devised, focusing on either direct access to **1** by hydroboration/oxidation (Figure 2B), or to **2** by Wacker oxidation of a terminal olefin (Figure 2C). Both strategies allow for access of either C13 epimer, as the relative configuration of the secondary alcohol at C13 of **2** was undetermined in the original isolation report. Hydroboration/ oxidation of **10** with either isomer of alkene (derived from tiglic or angelic acid) should afford **2**; similarly **1**, produced directly by Wacker oxidation of **13**, affords **2** by stereoselective reduction. Installation of the sidechain at C3 could be accomplished by enolate addition to the isochromanone carbonyl of **9** and **12** in both strategies and the isochromanone functionality would be produced by oxidation of the activated C3 of the isochroman. Stereoselective C–H insertion reactions proceed from aryl-hydrazones to form isochromans when subjected to chemoselective oxidation by MnO_2, followed by addition of dirhodium carboxylate catalysts. Notably, these two retrosynthetic approaches make use of aryl/methyl carbenes. Previous work in our lab with this type of carbene showed poor enantioselectivity when C–H insertion occurred at a benzylic site (60:40er), therefore posing a unique challenge in the synthesis.[27] While aryl/alkyl carbenes have been used in other C–H insertion reactions, to date none have been reported to be enantioselective.[29]

Based on previous efforts in our lab, it was expected that C–H insertion into allylic sites would achieve high enantioselectivity and high yields, making a hydroboration/ oxidation-based strategy attractive. Conversely, insertion reactions into relatively unactivated homoallylic C–H bonds to form isochromans are not as precedented for high yields and stereoselectivities, making a Wacker oxidation-based route the more challenging strategy.[27] As such, the hydroboration/oxidation route was pursued: acetophenones of both tiglyl (***E*-17)**

and angelyl (**Z-17)** substitution were accessed in a straightforward sequence from **14** and then converted to their corresponding hydrazones (Figure 3).

Screening of conditions for the C–H insertion reaction demonstrated a gratifying level of enantioselectivity for both alkene substrates (Table 1, entries 4 and 8, 93:7er), in stark contrast to the related prior result (60:40er). For ***E*-18**, optimal conditions were achieved in acetonitrile at −15 ºC with Rh_2(*R*-PTAD)$_4$. The analogous angelyl-derived substrate ***Z*-18** required a reduction in temperature (−78 ºC) to achieve the same selectivity, necessitating dichloromethane as the solvent. In both cases, insertion protocols were amenable to scale up, achieving comparable yields and enantioselectivities at 8 mmol (~2 g) with catalyst loading lowered by an order of magnitude.

As shown in Figure 4, the vinyl-isochroman insertion product ***Z*-19** was then oxidized at C3 with PCC to form the isochromanone in modest yield and the structure was confirmed by X-ray crystallography, confirming the stereochemical outcome expected per our previous reports.[27,30] The lithium enolate of *tert*-butyl acetate was then added to this lactone carbonyl to give hemi-acetal **20** which was isolated as a single diastereomer after chromatography. Diastereoselective reduction of **20** with BF_3•OEt_2 and triisopropylsilane then completed the assembly of isochroman **21**, the key intermediate for our planned synthesis of **1** and **2**. Several hydroboration reagents were screened to install the secondary alcohol required for **2**: BH_3•DMS provided **22** in 70% yield with 93:7dr as the best result. **22** was carried forward to the reduction of the pendant ester to complete the synthesis of **23**. Subsequent oxidation to the methyl ketone in a three step sequence produced **24**. For the angelyl-derived **23** and **24**, the NMR spectra were not in agreement with the reported natural materials **1** and **2**. Similarly unsatisfying, the synthesis was repeated starting from tiglyl-derived ***E*-15**, resulting in NMR spectra that were again not consistent with the natural substances **1** and **2** (not shown).[30]

To determine the relative and absolute stereochemistry of these panowamycin isomers, a crystal structure of the bis-*para*-nitro benzoate **25** was obtained. From this structure, it was shown that the angelyl-derived alkene underwent hydroboration/ oxidation with selectivity for 12-*epi*-panowamycin (Figure 5). Selectivity for the undesired C12 epimer in this case is rationalized by allylic-1,3 strain analysis. Conversely, the tiglyl-derived **4** was not spectroscopically consistent with **24**, nor **1**, implying that the tiglyl-derived substrate generated the and desired C12 configuration and that **1** was misassigned. The configuration of **4** was later confirmed by chemical correlation with TM-135. The hydroboration/oxidation of **26** was achieved in 40% yield and with 75:25dr; although several substituted boranes were explored in an effort to improve yield and selectivity, all failed to react with the trisubstituted alkene.[30] Therefore, while C–H insertion reactions using methyl/aryl carbenes were successfully optimized to stereoselectively generate the isochroman scaffolds, the hydroboration/oxidation was not suitable for our purposes.

Taking these challenges into account, the Wacker oxidation strategy was then pursued, as it allows for certainty of configuration at a pre-installed C12 stereogenic center (Figure 6). The requisite homoallylic alcohol **29** was difficult to access as a single enantiomer by reported methods.[31–35] As proof of concept and to confirm the relative stereochemistry

of **1** and **2**, a racemic synthesis was performed from commercially available (±)-2-methyl-but-3-enoic acid (**28**). Hydrazone (±)-**30** was accessed in three steps, as above (Figure 3), in similar efficiency.[30] When (±)-**30** was subjected to the previously optimized C–H insertion conditions for **19**, conversion to the azine byproduct **31** and minimal formation of the desired isochroman was observed. Azine is a potential byproduct when C–H insertion reactions are particularly slow. The reduced reactivity can be attributed to the lack of allylic activation and the presence of adjacent branching at the homoallylic insertion site. This reaction was circumvented by modifying the insertion protocol to an inverse addition sequence, limiting the relative concentrations of the diazo and metal-carbene species. Under these conditions, (±)-**30** was oxidized with MnO_2, the heterogenous oxidant was filtered, and the diazo-containing solution was added dropwise by syringe pump over three hours to a dilute solution of dirhodium catalyst (0.5 mol %).[30] This modified procedure suppressed azine formation and enabled isolation of the desired isochroman (±)-**32** in 65% yield.

Due to the high diastereoselectivity of the C–H insertion reaction (>95:5 *cis*:*trans* at C10 and C11) and the presence of the distal stereogenic center, the racemic hydrazone led to a 50:50 mixture of isochroman diastereomers (Figure 6). While inseparable at (±)-**32**, these diastereomers were cleanly separated after PCC oxidation to their respective chromanones. (±)-**34** was then accessed from isochromanone (±)-**12** as shown in Figure 4. The pendant ester was reduced with $LiAlH_4$ and the subsequent intermediate was subjected to Wacker oxidation conditions, producing methyl-ketone (±)-**4** in 94% yield. However, the NMR spectra were again inconsistent with those reported for **1**. Reduction of the ketone, on the other hand, gave a 75:25dr of diol (±)-**5**, where the major isomer *matched* the NMR spectra for **2**. Both isomers were acylated to improve crystallinity and a structure of the minor isomer was obtained by X-ray crystallography.[30] This structure allowed for the confirmation of the relative stereochemistry at C12 and C3 reported in the original assignment by Ōmura and coworkers, therefore proving the misassignment of **1**. This structure also proved the relative configuration of C12 and C13 allowing for the stereochemical assignment of panowamycin B (**2**) as **5**.

In order to predict the likely stereochemical identity of panowamycin A, theoretical NMR calculations were performed for the eight potential diastereomers of **1** (Table 2, only **1** and **3** are shown, see SI for other structures). The PCM(chloroform)-mPW1PW1/6–311+G(2d,p)//B3LYP-D3(BJ)/6–31+G(d,p)[36–42] level of theory was used with the GIAO method[43–47] of calculating isotropic shielding constants. From these calculations of both ^{1}H and ^{13}C chemical shifts (see SI for the full ^{1}H and ^{13}C chemical shift tables), **3** had the lowest mean absolute deviation (MAD) (Table 2). Additionally, isomer **3** was the only isomer where all of the absolute chemical shift deviations for both ^{1}H and ^{13}C nuclei were within the tolerated deviations for this method (<0.3 ppm for ^{1}H shifts; <7 ppm for ^{13}C shifts).[48] DP4 analysis was performed for the four isomers with the lowest MADs to give the probability of each isomer being the natural isomer.[49] Using ^{1}H and ^{13}C chemical shifts with the DP4-database2 (with t-distribution), **3** was predicted to have a 99.9% probability of being the natural product, whereas **1** was predicted to have only a 0.1% probability.[30]

With this computational analysis suggesting **3** as the natural substance, a second-generation synthesis of the homoallylic scaffold was investigated (Figure 7). Benzyl alcohol **35** was

converted into the corresponding trichloroacetimidate which was alkylated with *S*-Roche ester under acidic conditions. This ester was then reduced, oxidized, and subjected to Wittig conditions in an efficient sequence to generate chiral homoallylic ether **37**. The subsequent hydrazone **30** was obtained as above and the two-pot, inverse addition C–H insertion conditions were optimized to produce **32** in 80:20dr and 79% yield. The observed diastereoselectivity is the result of catalyst induction in the insertion step, where good selectivity between **32** and **39** is achieved while C10-C11 *cis*-selectivity is still >95:5. Other commercially available dirhodium carboxylate catalysts gave inferior diastereoselectivity compared to Rh_2(*S*-TCPTTL)$_4$ and also increased amounts of azine byproduct **31**. Yields, selectivities, and relative amounts of azine fluctuated slightly with changes in scale, but the process was amenable to 8 mmol scale (~2 g) and 0.5 mol % catalyst.[30]

The stereoselective construction of this isochroman scaffold then allowed for the asymmetric synthesis of panowamycin A in 5 steps from **32**. PCC oxidation of C3 was again successful and the diastereomers of **12** resulting from the prior insertion step were separated. To invert the stereoselective outcome at C3 and access **3** rather than **1**, the isochromanone carbonyl was first reduced to the hemi-acetal and acetylated *in situ*. When treated with BF_3•OEt_2, **40** formed an oxocarbenium species that was attacked by silylketene acetal **41** with facial selectivity for the *si* face, affording **42**. Reduction of the pendant ester and Wacker oxidation produced **3**, the isomer predicted by computational NMR to be panowamycin A. This compound's NMR spectra matched those of Ōmura, affirming our computational prediction and completing the asymmetric synthesis of panowamycin A. Reduction of **3** afforded crystalline diol **43** as the minor diastereomer and the absolute and relative configuration of **3** at C12 and C3 were therefore confirmed by X-ray crystallography. Reaffirming our assignment of panowamycin B as **5** (Figure 6), neither diastereomer from this reduction of **3** was spectroscopically consistent with Ōmura's panowamycin B.[30]

Contemporaneous with our syntheses, Mahmud and coworkers published their detailed work on the isolation and biological testing of panowamycin A from *Streptomyces pactum* ATCC 27456.[14] In their report, they performed an updated analysis of the NMR spectra for panowamycin A, concluding that the configuration at C3 is the same that was proposed by our NMR computations. CD spectroscopy performed in that study on stereochemically related molecules (TM-131, TM-132) also proposed the absolute stereochemistry for panowamycin A. Interestingly, Mahmud and coworkers also isolated TM-135 (**4**), which corresponds to the originally proposed relative stereochemical assignment of **1** by Ōmura. These findings suggest that NFAT-133 (**6**), the likely biological precursor for panowamycin A and TM-135, can cyclize from either *re* or *si* faces to form these natural products, respectively. By comparison to the NMR spectra of Mahmud's TM-135, our synthetic **4** (Figure 5 and 6) was determined to be spectroscopically consistent with their natural substance.

With these data from Mahmud and coworkers, we pursued the divergent *asymmetric* synthesis of TM-135 (**4**), and subsequently panowamycin B (**5**), from isochromanone **12** (Figure 7). Ketone **4** was accessed from **12** as single diastereomer using the enolate addition/ reduction sequence developed in Figure 6. Stereoselective reduction of **4** was achieved with

$LiAlH_4$, affording **5** in 67% yield and 75:25dr, thereby also completing the asymmetric synthesis of TM-135 and panowamycin B. Interestingly, optical rotation measurements for panowamycin A and TM-135 are consistent with Ōmura and Mahmud in both sign and magnitude (confirming Mahmud's proposed absolute configuration), while panowamycin B was measured to be the *opposite* sign with similar magnitude.[30] Although it is possible that we have synthesized *ent*-panowamycin B, we consider it unlikely that this natural product would not conserve the three adjacent stereocenters shared by **3**, **4**, and **6.** And while the major diastereomer from the reduction of **3** in Figure 7 (not shown) has a more similar sign and magnitude when compared to Omura measurements, their NMR spectra are noticably incongruent.[30] Futhermore, ketones **3**, **4**, and **24** maintain the same sign as their diol analogues (both diastereomers).[30]

Schäberle and Bauer recently reported the isolation of a new polyketide natural product, veramycin F (**46**), from *Streptomyces* sp. ST157608, which features the same isochroman core as the panowamycins and TM-135.[8] Taking advantage of intermediate **12**, a Wacker oxidation produced **44**, which was not spectroscopically consistent with veramycin F (Figure 8). Lactone **45**, derived from C–H insertion minor isomer **39**, was also oxidized to produce **46**, which matched the NMR spectrum reported in the isolation publication, thereby completing the asymmetric synthesis and structural reassignment of the relative configuration of veramycin F (**46**). Interestingly, veramycin F contains a different relative configuration compared to the other related natural products isolated in their report (i.e. NFAT-133, panowmaycins, benwamcyins, TM-123). Under biological conditions, it is possible that the relatively acidic protons *alpha* to the ketone of **44** could epimerize to form *ent*-**46**.

In conclusion, we report the first synthesis of panowamycins A and B, as well as TM-135 and veramycin F through a common intermediate. These syntheses were accomplished asymmetrically by a C–H insertion reaction using a donor/donor carbene in the key bond-forming step. Having synthesized the originally proposed structure of **1**, we determined that Ōmura and coworkers had misassigned the structure of panowamycin A. Using NMR chemical shift computations, we predicted the structure of the natural substance, which was later confirmed to be correct by synthesis and NMR spectra comparison. Contemporaneous reports by Mahmud and coworkers provide independent support of these computational and synthetic efforts by an updated NMR analysis of their isolated samples of **3**. In this way, we report the unambiguous determination of the relative and absolute configuration of these natural products, thus enabling future studies of their biological activity.

Supplementary Material

Refer to Web version on PubMed Central for supplementary material.

Acknowledgements

This work was supported by grants from the National Institutes of Health (R01/GM124234) and National Science Foundation (XSEDE). We acknowledge the MPS computing cluster (Peloton) at UC Davis. We also thank the National Science Foundation (Grant CHE-1531193) for the Dual Source X-ray diffractometer.[50] BDB and JTS acknowledge Prof Dr. Satoshi Ōmura, Prof. Dr. Taifo Mahmud, and Dr. Armin Bauer for supplying NMR spectra for their natural product isolates. BDB and JTS acknowledge the Franz and Olson labs (UC Davis) for the use

of their Chiral HPLC and FTIR instruments, respectively. We also thank Dr. William T. Jewell (UC Davis) for assistance with mass spectrometry. BDB thanks UC Davis for support in the form of Borge and Corson/DOW fellowships.

References

[1]. Li DY, Wei JX, Hua HM, Li ZL, J. Asian Nat. Prod. Res. 2014, 16, 1018–1023. [PubMed: 24993137]

[2]. Li XH, Han XH, Qin LL, He JL, Cao ZX, Gu YC, Le Guo D, Deng Y, Nat. Prod. Res. 2019, 33, 1870–1875. [PubMed: 29792356]

[3]. Kock I, Draeger S, Schulz B, Elsässer B, Kurtán T, Kenéz Á, Antus S, Pescitelli G, Salvadori P, Speaknian JB, et al., European J. Org. Chem. 2009, 9, 1427–1434.

[4]. Li W, Bin Yang Y, Yang XQ, Xie HD, Shao ZH, Zhou H, Miao CP, Zhao LX, Ding ZT, Planta Med. 2017, 83, 654–660. [PubMed: 27806408]

[5]. Ogawa A, Murakami C, Kamisuki S, Kuriyama I, Yoshida H, Sugawara F, Mizushina Y, Bioorganic Med. Chem. Lett. 2004, 14, 3539–3543.

[6]. Zhang L, Zhu X, Zhao BX, Zhao J, Zhang Y, Zhang SL, Miao JY, Vascul. Pharmacol. 2008, 48, 63–69. [PubMed: 18299254]

[7]. Liu J, Birzin ET, Chan W, Yang YT, Pai LY, DaSilva C, Hayes EC, Mosley RT, DiNinno F, Rohrer SP, et al., Bioorganic Med. Chem. Lett. 2005, 15, 715–718.

[8]. Dardić D, Böhringer N, Plaza A, Zubeil F, Pohl J, Sommer S, Padva L, Becker J, Patras MA, Bill M-K, et al., Org. Chem. Front. 2022, 9, 1604–1615.

[9]. Hashida J, Niitsuma M, Iwatsuki M, Mori M, Ishiyama A, Namatame M, Nishihara-Tsukashima A, Matsumoto A, Ara I, Takahashi Y, et al., J. Antibiot. 2012, 65, 197–202.

[10]. Yang FX, Huang JP, Liu Z, Wang Z, Yang J, Tang J, Yu Z, Yan Y, Kai G, Huang SX, J. Nat. Prod. 2020, 83, 111–117. [PubMed: 31904958]

[11]. Sato H, Kwon E, Taguchi Y, Yoshida S, Kuwahara S, Ogura Y, J. Nat. Prod. 2019, 82, 1791–1796. [PubMed: 31268714]

[12]. Yang Y, Yu L, Komaki H, Oku N, Igarashi Y, J. Antibiot. 2016, 69, 69–71.

[13]. Zhou W, Posri P, Abugrain ME, Weisberg AJ, Chang JH, Mahmud T, ACS Chem. Biol. 2020, 15, 3217–3226. [PubMed: 33284588]

[14]. Zhou W, Posri P, Liu X-J, Ju Z, Lan W-J, Mahmud T, J. Nat. Prod. 2021, 84, 2411–2419. [PubMed: 34519213]

[15]. Larghi EL, Kaufman TS, Synthesis 2006, 2, 187–220.

[16]. Larghi EL, Kaufman TS, European J. Org. Chem. 2011, 27, 5195–5231.

[17]. Tamanna M.Kumar, Joshi K, Chauhan P, Adv. Synth. Catal. 2020, 362, 1907–1926.

[18]. Das S, Liu L, Zheng Y, Alachraf MW, Thiel W, De CK, List B, J. Am. Chem. Soc. 2016, 138, 9429–9432. [PubMed: 27457383]

[19]. Zhao C, Chen SB, Seidel D, J. Am. Chem. Soc. 2016, 138, 9053–9056. [PubMed: 27396413]

[20]. Doyle MP, Van Oeveren A, Westrum LJ, Protopopova MN, Clayton TW Jr., J. Am. Chem. Soc. 1991, 113, 8982–8984.

[21]. Doyle MP, Dyatkin AB, J. Org. Chem. 1995, 60, 3035–3038.

[22]. Davies HML, Grazini MVA, Aouad E, Org. Lett. 2001, 3, 1475–1477. [PubMed: 11388845]

[23]. Davies HML, Hansen T, J. Am. Chem. Soc. 1997, 119, 9075–9076.

[24]. Davies HML, Hansen T, Churchill MR, J. Am. Chem. Soc. 2000, 122, 3063–3070.

[25]. Ye T, McKervey MA, J. Chem. Soc., Chem. Commun. 1992, 823–824.

[26]. Ito M, Kondo Y, Nambu H, Anada M, Takeda K, Hashimoto S, Tetrahedron Lett. 2015, 56, 1397–1400.

[27]. Nickerson LA, Bergstrom BD, Gao M, Shiue YS, Laconsay CJ, Culberson MR, Knauss WA, Fettinger JC, Tantillo DJ, Shaw JT, Chem. Sci. 2020, 11, 494–498. [PubMed: 32874491]

[28]. Paterson I, Lam NYS, J. Antibiot 2018, 71, 215–233.

[29]. Bergstrom BD, Nickerson LA, Shaw JT, Souza LW, Angew. Chemie - Int. Ed 2020, 60, 6864–6878.
[30]. See Supporting Information, n.d.
[31]. Normandin C, Malouin F, Marsault E, European J. Org. Chem. 2020, 18, 2693–2698.
[32]. Padarti A, Kim D, Han H, Org. Lett. 2018, 20, 756–759. [PubMed: 29345942]
[33]. Poremba KE, Lee VA, Sculimbrene BR, Tetrahedron 2014, 70, 5463–5467.
[34]. Sengupta A, Hosokawa S, Tetrahedron Lett. 2019, 60, 411–414.
[35]. Li H, Wu J, Luo J, Dai WM, Chem. Eur. J. 2010, 16, 11530–11534. [PubMed: 20803588]
[36]. Adamo C, Barone V, J. Chem. Phys. 1998, 108, 664–675.
[37]. Becke AD, J. Chem. Phys. 1993, 98, 5648–5652.
[38]. Tomasi J, Mennucci B, Cammi R, Chem. Rev. 2005, 105, 2999–3093. [PubMed: 16092826]
[39]. Frisch MJ, Pople JA, Binkley JS, J. Chem. Phys. 1984, 80, 3265–3269.
[40]. Clark T, Chandrasekhar J, Spitznagel GW, Schleyer PVR, J. Comput. Chem. 1983, 4, 294–301.
[41]. Grimme S, Antony J, Ehrlich S, Krieg H, J. Chem. Phys. 2010, DOI 10.1063/1.3382344.
[42]. Grimme S, Ehrlich S, Goerigk L, J. Comput. Chem. 2011, DOI 10.1002/jcc.21759.
[43]. London F, J. Phys. Radium 1937, 8, 397–409.
[44]. McWeeny R, Phys. Rev. 1962, 126, 1028–1034.
[45]. Ditchfield R, Mol. Phys. 1974, 27, 789–807.
[46]. Wolinski K, Hinton JF, Pulay P, J. Am. Chem. Soc. 1990, 112, 8251–8260.
[47]. Cheeseman JR, J. Chem. Phys. 1996, 104, 5497–5509.
[48]. Lodewyk MW, Siebert MR, Tantillo DJ, Chem. Rev. 2012, 112, 1839–1862. [PubMed: 22091891]
[49]. Smith SG, Goodman JM, J. Am. Chem. Soc. 2010, 132, 12946–12959. [PubMed: 20795713]
[50]. See CCDC database 2143756, 2143757, 2143758, 2143759

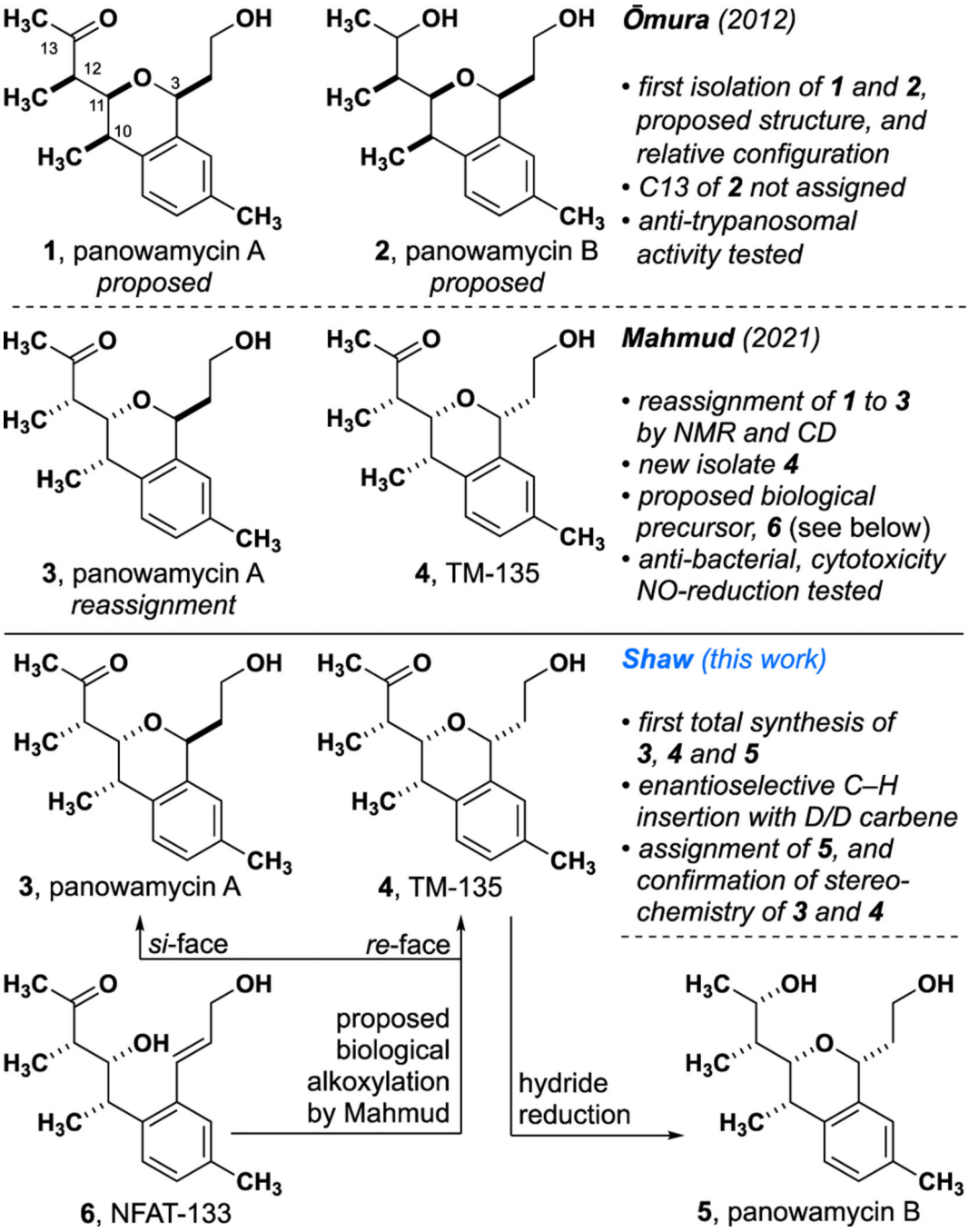

Figure 1.
The first total synthesis of the isochroman natural products isolated by Ōmura and Mahmud

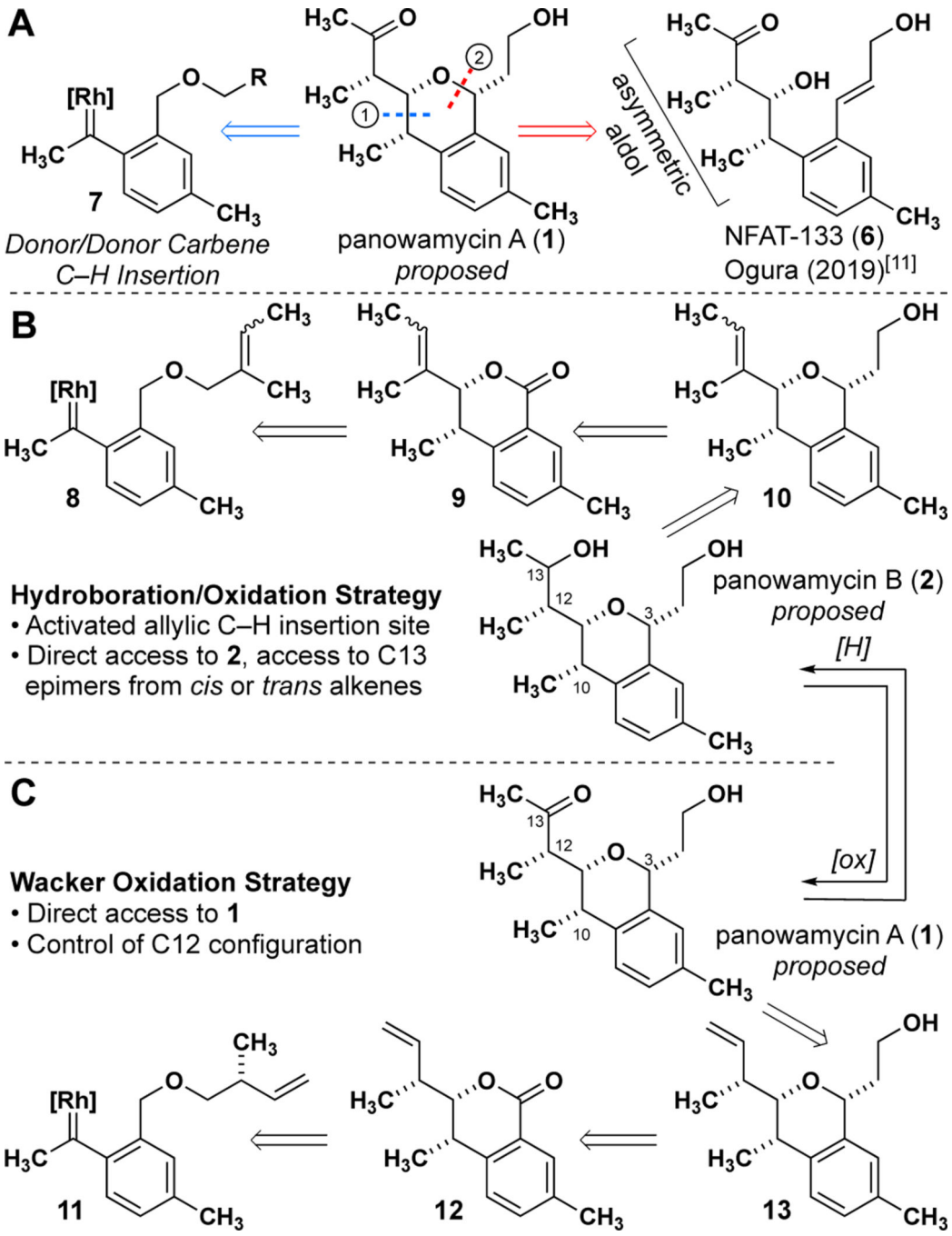

Figure 2.

A: C–O disconnection versus C–C disconnection for **1**, B: retrosynthetic strategy for **2**, C: retrosynthetic strategy for **1**

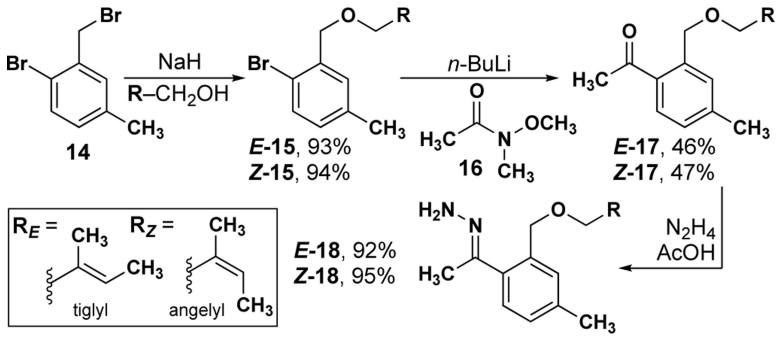

Figure 3.
Synthesis of acetophenone hydrazone intermediates

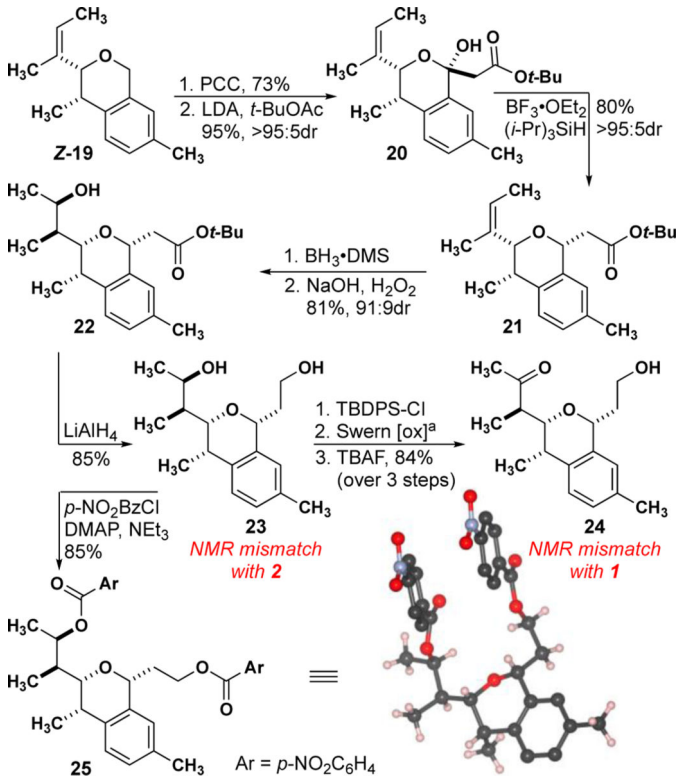

Figure 4.

Synthesis of 12-*epi*-panowamycin A and B from angelyl-derived ***Z*-15** [a](COCl)$_2$, DMSO, NEt$_3$

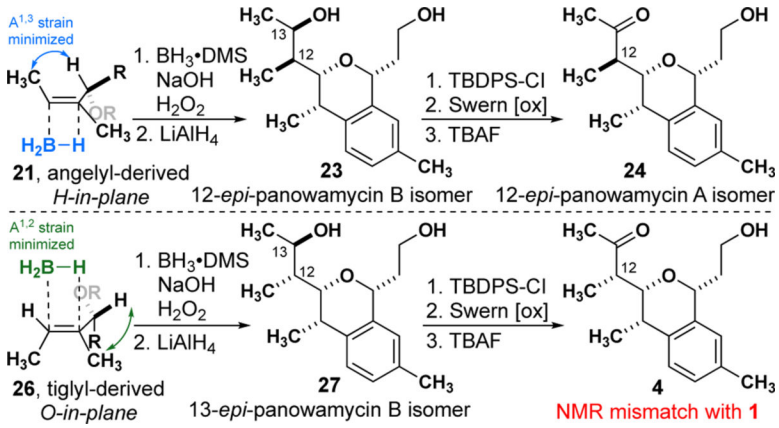

Figure 5.

Allylic-1,3 and allylic-1,2 strain analysis of angelyl/tiglyl-derived substrates for hydroboration/oxidation

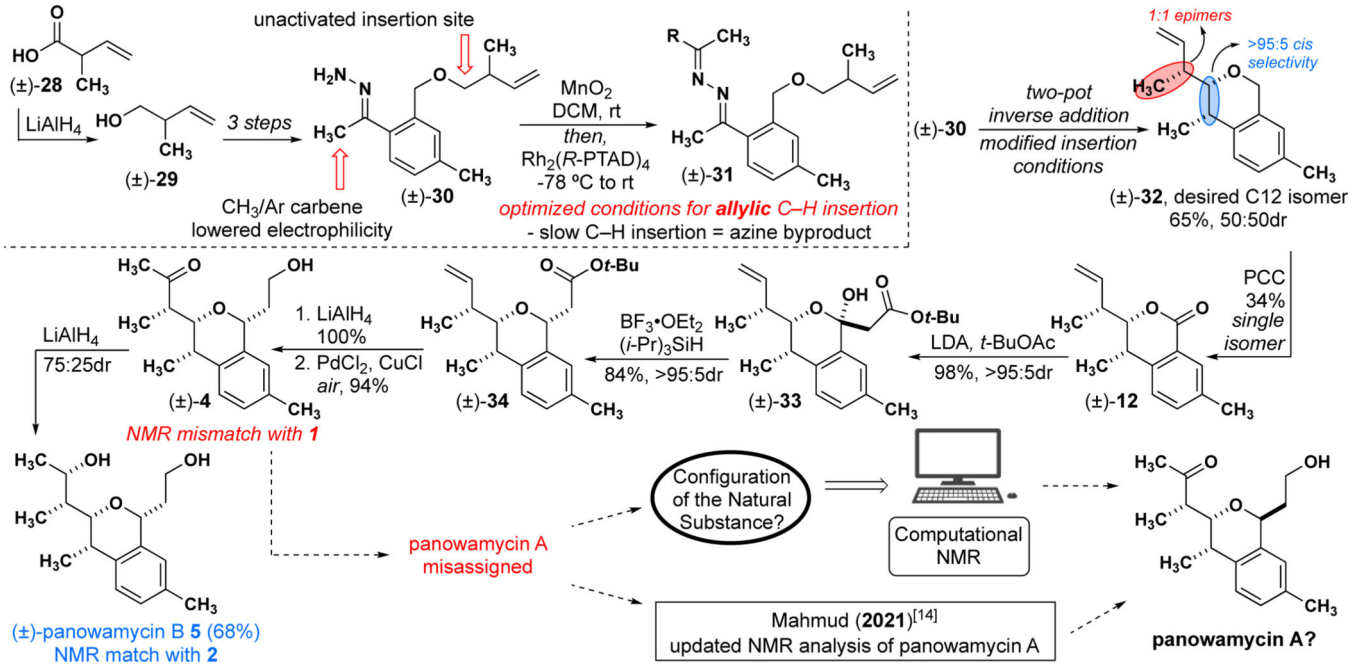

Figure 6.

Modified insertion protocol to limit azine byproduct formation; the racemic synthesis of the proposed structure of 1 and confirmation of misassignment

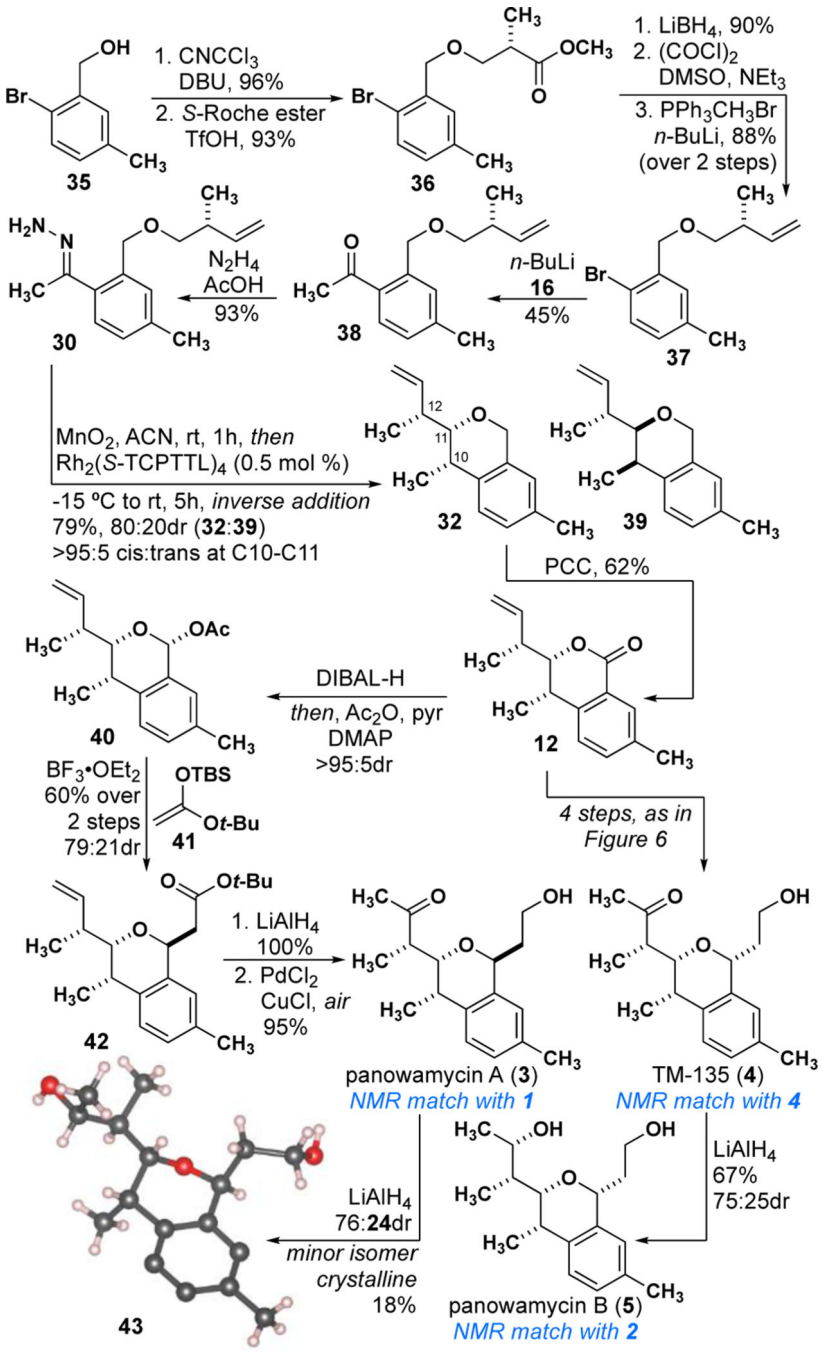

Figure 7.

Divergent, asymmetric total synthesis of panowamycin A, B, and TM-135 using the Roche ester

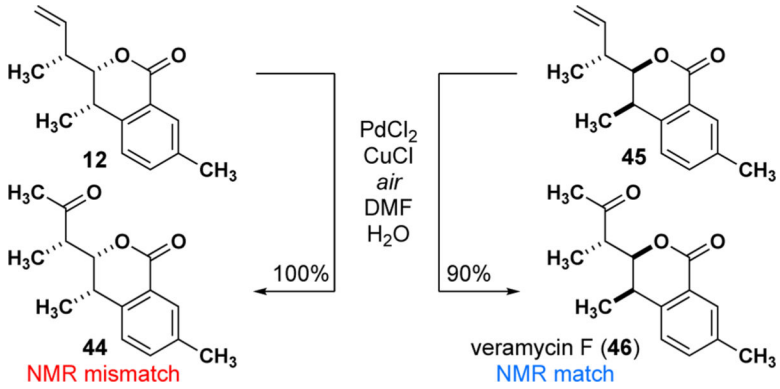

Figure 8.
Asymmetric synthesis of veramycin F by Wacker oxidation

Table 1.

Donor/Donor carbene allylic C–H insertion optimization

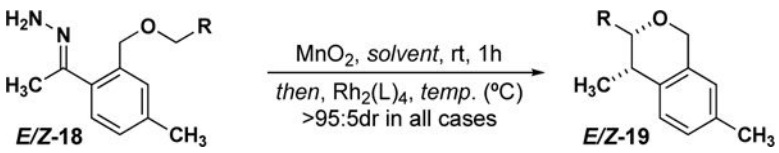

entry	18	temp	solvent	catalyst[a]	er	yield (%)
1	*E*	−20	ACN	Rh_2(*R*-PTAD)$_4$	17:83	94
2	*E*	−20	ACN	Rh_2(*R*-PTAD)$_4$ [b]	10:90	69
3	*E*	−20	ACN	Rh_2(*R*-BTPCP)$_4$	81:19	56
4	*E*	−20	ACN	Rh_2(*S*-TCPTTL)$_4$	93:7	65
5	*Z*	−20	DCM	Rh_2(*S*-TCPTTL)$_4$	86:14	83
6	*Z*	−45	DCM	Rh_2(*S*-TCPTTL)$_4$	92:8	85
7	*Z*	−78	DCM	Rh_2(*R*-PTAD)$_4$ [b]	7:93	79

[a] 0.1 mmol scale and 1 mol % catalyst loading

[b] 8 mmol scale and 0.07 mol % catalyst loading

Table 2.

Computed NMR chemical shifts of panowamycin isomers compared to the natural substance shifts

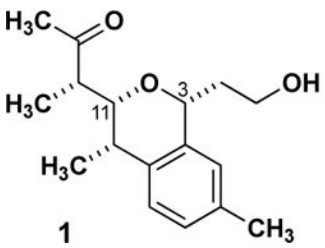

1

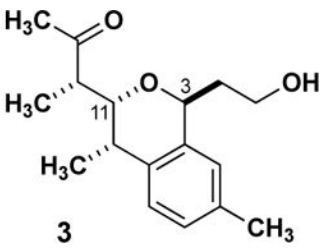

3

isomer	Abs. Dev. (ppm)				MAD[a] (ppm)	
	C3	C11	H3	H11	C	H
A (**1**)	7.3	5.6	0.08	0.15	**1.7**	**0.14**
B	6.1	9.0	0.03	0.31	2.1	0.15
C	6.4	7.4	0.12	0.07	2.2	0.14
D	5.5	8.5	0.00	0.10	2.1	0.14
E (**3**)	4.9	0.2	0.05	0.25	**1.2**	**0.08**
F	0.6	7.1	0.00	0.06	2.0	0.14
G	1.2	1.7	0.38	0.24	1.9	0.18
H	1.3	6.9	0.08	0.17	2.3	0.15

[a]MAD = Mean Absolute Deviation, for all chemical shift values of each respective isomer. See supporting information for isomer structures.